

Gravito-diamagnetic forces for mass independent large spatial superpositions

Run Zhou,¹ Ryan J. Marshman,² Sougato Bose,³ and Anupam Mazumdar¹

¹*Van Swinderen Institute, University of Groningen, 9747 AG Groningen, The Netherlands.*

²*Centre for Quantum Computation and Communication Technology, School of Mathematics and Physics, University of Queensland, Brisbane, Queensland 4072, Australia*

³*Department of Physics and Astronomy, University College London, Gower Street, WC1E 6BT London, United Kingdom.*

(Dated: December 6, 2022)

Testing the quantum nature of gravity in a laboratory via entanglement requires us to create a massive spatial quantum superposition, i.e. the Schrödinger cat state, where the mass and the superposition ought to be around $10^{-15} - 10^{-14}$ kg and $\Delta x \sim 10 - 100$ μm . Creating such a massive spatial quantum superposition poses incredible challenges. The methods employed so far rely either on wavepacket expansion or on a quantum ancilla, e.g. single spin dependent forces, scale inversely with mass (e.g. force per unit time has to be proportionately enhanced). In this paper, we will show that gravitational acceleration along with the diamagnetic repulsion can achieve a complete “release” and “catch” interferometry in the course of which a large spatial superposition is generated in a relatively short time. After first creating a modest initial spatial superposition 1 μm (e.g. using Stern-Gerlach), we will show that we can achieve an $\sim 10^3$ fold improvement to the spatial superposition size (1 $\mu\text{m} \rightarrow 965$ μm) between the wave packets in *just* 0.034 s by using the Earth’s gravitational acceleration and then the diamagnetic repulsive scattering of the nanocrystal, neither of which depend on the object mass. In fact, we will be able to slow down the wavepackets to almost zero velocities before we can capture them in the Stern-Gerlach apparatus to close the interferometer.

Introduction: Gravity could be a classical, or an emergent or a quantum entity [1]. There is no experimental proof to ascertain the quantum nature of gravity in a laboratory [2]. It is pertinent to ask how to show the quantum nature of gravity in a laboratory. Recently the quantum protocol has been established to explore the quantum origin of gravity with the help of quantum superposition and quantum entanglement in the infrared [3–6], see also for a similar proposal [7]. Note that the entanglement is inherently a quantum entity, and has no classical analogue. The protocol is known as the quantum gravity induced entanglement of masses (QGEM), which evidences both quantum superposition of geometries [8, 9], and the exchange of massless spin-2 graviton [5, 6, 10], that is, the massless excitation of spin-2 graviton. A protocol has also been created to entangle the matter with that of the Standard Model photon in a gravitational optomechanical setup [11], see also [12], which probes the light bending due to the gravitational interaction and also constrain the spin-2 nature of the graviton mediated entanglement [11].

To realise the QGEM protocol experimentally is extremely challenging, we will need to create a large spatial superposition $\Delta x \sim O(10-100)$ μm for a large mass object $m \sim O(10^{-15} - 10^{-14})$ kg, see for details in [3, 13] in a free falling setup [3, 14]. Creating a macroscopic quantum superposition has many other fundamental applications; testing very foundation of quantum mechanics in presence of gravity [15–19], equivalence principle [20], placing the bound on the decoherence mechanisms [21–27], quantum sensors [14, 28], probing fifth force [29], and detecting gravitational waves [28]. Atom interferometers have al-

ready created a large baseline superposition [30–32], but at masses well below what is required to test the quantum nature of gravity. To date, macromolecules represent the heaviest masses placed in a superposition of spatially distinct states [33, 34]. There are many physical schemes to obtain tiny superpositions of large masses [35] for 10 nm – 1 μm superposition for $m \sim 10^{-19} - 10^{-17}$ kg [22, 23, 36–47]. However, the QGEM proposal requires a large spatial superposition and heavy masses. For this reason the scheme will likely be utilising the Stern-Gerlach (SG) effect [48–50]. A proof of principle experiment has already been performed using atoms [51]. However, the critical challenge is how to achieve a large spatial superposition, and whether it is possible to benefit from Earth’s gravitational acceleration when creating the superposition.

There are already a couple of experimental schemes for creating large spatial superposition state for massive objects [51–53], but these schemes inevitably become progressively less effective as the mass increases. However, we have recently shown that it is possible to provide a mass-independent scheme to enhance the spatial superposition from the initial superposition size of ~ 1 μm with the help of diamagnetic repulsion [54]. The aim of this paper will be to illustrate how such a mass-independent scheme of diamagnetic repulsion can benefit by utilising Earth’s gravitational acceleration in a unique way to create even quicker enhancement of $O(965)$ μm in 0.034 s.

Mass-independent acceleration: We assume that the experimental apparatus is fixed in the Earth’s gravitational field. The Hamiltonian of a nanodiamond with a nitrogen-vacancy (NV) centre spin

embedded in presence of an external magnetic field is given by: [38, 42]

$$\hat{H} = \frac{\hat{\mathbf{p}}^2}{2m} + \hbar D \hat{\mathbf{S}}^2 - \hat{\boldsymbol{\mu}} \cdot \mathbf{B} + mg\hat{z} - \frac{\chi_\rho m}{2\mu_0} \mathbf{B}^2. \quad (1)$$

The first term in Eq.(1) represents the kinetic energy of the nanodiamond, $\hat{\mathbf{p}}$ is the momentum operator and m is the mass of the nanodiamond. The second term represents the zero-field splitting of the NV centre with $D = (2\pi) \times 2.8$ GHz, \hbar is the reduced Planck constant and $\hat{\mathbf{S}}$ is the spin operator of the NV electron spin. The third term represents the interaction energy of the NV electron spin magnetic moment with the magnetic field \mathbf{B} . Spin magnetic moment operator $\hat{\boldsymbol{\mu}} = -g_s\mu_B\hat{\mathbf{S}}$, where $g_s \approx 2$ is the Landé g-factor and $\mu_B = e\hbar/2m_e$ is the Bohr magneton. The fourth term is the gravitational potential energy, $g \approx 9.8$ m/s² is the gravitational acceleration and \hat{z} is the position operator along the direction of gravity (z axis). The final term represents the magnetic energy of a diamagnetic material (nanodiamond) in a magnetic field, $\chi_\rho = -6.2 \times 10^{-9}$ m³/kg is the mass susceptibility and μ_0 is the vacuum permeability.

We will first assume that an initial superposition state with a small spatial separation has been obtained by the SG apparatus [51–53], and then apply a microwave pulse to couple the electron spin to the nuclear spin so that the spin magnetic field interaction can be ignored [55, 56]. Therefore, by neglecting the spin magnetic field interaction, the potential energy in Eq.(1) reduces to:

$$U = mg\hat{z} - \frac{\chi_m m}{2\mu_0} \mathbf{B}^2. \quad (2)$$

To facilitate the separation of the wave packets by using the diamagnetic repulsion, we will consider the central magnetic field generated by the current-carrying wire

$$\mathbf{B} = \frac{\mu_0 \mathbf{I} \times \mathbf{e}_r}{2\pi r}, \quad (3)$$

where \mathbf{I} is the current carried by a straight wire. r is the radius from a point in space to the centre of the wire. \mathbf{e}_r is the unit vector corresponding to the radius r . Combining Eq.(2) and Eq.(3), we can obtain the acceleration of the nanodiamond as follows

$$\mathbf{a}_{dia} = -\frac{1}{m} \nabla U = -g\mathbf{e}_z + \alpha \frac{I^2}{r^3} \mathbf{e}_r, \quad (4)$$

where $\alpha = -\frac{\chi_m \mu_0}{4\pi^2}$. \mathbf{e}_z is the unit vector along the positive z axis. Note that Eq.(4) the acceleration is independent of the mass. This property provides an excellent possibility of obtaining a large superposition size for a massive quantum object. If we define the straight wire be perpendicular to the $x-z$ plane and take the nanodiamond to start to fall from rest, then

the motion of the nanodiamond will be only in the $x-z$ plane.

Scattering processes: The experimental scheme is divided into two stages (see Fig.1). The first stage (Stage-I) serves to enhance the spatial superposition. The second stage (Stage-II) returns the spatial superposition to its initial state. The purpose of restoring the initial state is to close the trajectories of the wave packets with the SG apparatus and then recover the spin coherence [53]. Stage-I is divided into two parts. The first part is to use the mass-independent gravitational acceleration to accelerate the nanodiamond. By controlling the falling height one can control the speed of the nanodiamond. The second part is to use the mass-independent diamagnetic acceleration (the second term on the right-hand side of Eq.(4)) to change the velocity direction of the nanodiamond. If the initial positions of the two wave packets in the superposition are symmetric about the wire, then they can change their velocity direction in the opposite directions and thus a large spatial separation can be obtained, as shown in Fig.1.

The second stage of restoring the initial state is achieved by placing the current-carrying wires (left and right wires in Fig.1) at the appropriate places so that the nanodiamond is scattered again with the magnetic field and returns to its initial position along its original trajectory. We will show analytically the process by which the nanodiamond is accelerated by the gravitational field and then scattered elastically by the magnetic field generated by the current-carrying wire, and then numerically calculate the trajectory of the wave packet to verify the analytical results.

Analytical treatment: We will assume that the nanodiamond is accelerated by gravity from the rest at a distance from the wire and the effect of diamagnetic repulsion on the nanodiamond can be ignored at the initial stages of the free-fall. We will set the distance z_0 at which the nanodiamond is accelerated by gravity. The initial velocity of the nanodiamond derived by the gravitational acceleration is given by

$$\mathbf{v}_{in} = \sqrt{2z_0 g} \mathbf{e}_z. \quad (5)$$

We will now consider the process of a nanodiamond incident at a velocity \mathbf{v}_{in} , and then scattered by the magnetic field generated by the current-carrying wire. This scattering process can be solved analytically, see [54]. The scattering angle of the nanodiamond scattered by the central magnetic field is given by [54]

$$\theta_s = \left(1 - \frac{1}{\sqrt{k}}\right)\pi, \quad (6)$$

where

$$k = 1 + \alpha \frac{I^2}{v_{in}^2 b^2}. \quad (7)$$

Here b is the impact parameter. The geometric picture of θ_s and b is shown in Fig.1b. We will assume that the scattering angle θ_s is greater than $\pi/2$. The distance that the nanodiamond moves in the x -direction when it reaches its highest point is given by:

$$x_{\text{split}} = -\frac{1}{2} \frac{v_{in}^2}{g} \sin(2\theta_s), \quad (8)$$

and the superposition size is

$$\Delta x = 2x_{\text{split}} = -\frac{v_{in}^2}{g} \sin(2\theta_s). \quad (9)$$

When $\theta_s = 3\pi/4$, Δx achieves the maximum value v_{in}^2/g , and the current and impact parameter satisfy the relationship

$$\frac{I}{b} = v_{in} \sqrt{\frac{15}{\alpha}}. \quad (10)$$

When the nanodiamond reaches its highest point it scatters again with the magnetic field and then returns to its initial position along its original path, this can be achieved in a very similar manner, see also [54]. The total time taken for the nanodiamond to start falling from the rest and to return to its initial position is given by:

$$t_{\text{total}} = (2 + \sqrt{2}) \frac{v_{in}}{g}. \quad (11)$$

Numerical results: We will use the equation of motion, Eq.(4), to numerically solve for the trajectory of the wave packet. The numerical results are shown in Fig.1. We set the initial separation between wave packets $\Delta x_0 = 1 \mu\text{m}$ ($b = 0.5 \mu\text{m}$) and the initial coordinates of the expectation values of the positions of the two wave packets to be $(\pm 0.5, 490) \mu\text{m}$. The coordinate of the splitting wire is $(x = 0, z = 0) \mu\text{m}$ and the current through it, which is determined by Eq.(10), is 13.5089 A. The coordinates of the left and right wires are $(\pm 490, 245) \mu\text{m}$. We adjust the currents through the left and right wires so that the wave packet can return to its initial position¹. The current through the left and right wires are 37.8519 A. All three wires are switched on during the movement of the wave packets.

With the initial conditions we have set, the total dynamical time required for the nanodiamond to start falling from the rest and to return to its initial

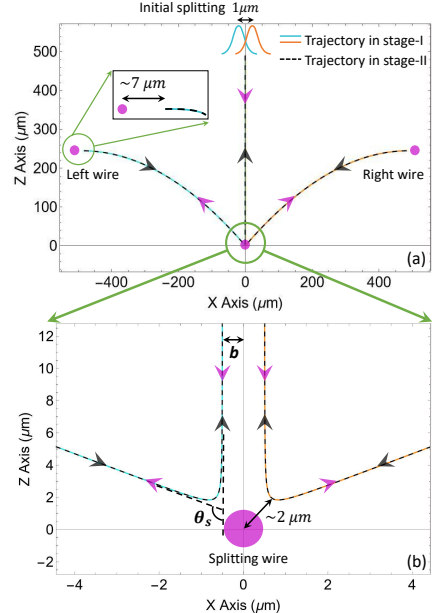


FIG. 1. We show the experimental scheme to create mass independent spatial superposition. The two wave packets with an initial spatial splitting of Δx_0 start falling, *under Earth's gravity acting along the $-z$ direction*, from the rest and enter the magnetic field generated by the current-carrying wires. The purple points represent straight wires perpendicular to the $x - z$ plane. The wire at the origin is called the *splitting wire* located at $(x = 0, z = 0)$. The wire on the left is called the *left wire* and the wire on the right is called the *right wire*. The blue and orange solid lines represent the wave packet trajectory in stage-I and the black dashed lines represent the wave packet trajectory in stage-II. The purple arrows indicate the direction of motion of the wave packets in the stage-I and the black arrows indicate the direction of the motion of the wave packet in the stage-II. Fig.1(a) shows the numerical trajectories of the wave packets in the gravitational and the magnetic fields, and Fig.1(b) shows their magnified image near the splitting wire. The sign b is the impact parameter and the initial splitting $\Delta x_0 = 2b = 1 \mu\text{m}$. The sign θ_s is the scattering angle. The total motion time is around 0.034 s.

position is about 0.034 s, which agrees well with the analytical expression Eq.(11). In the process of separating and then recombining the two wave packets, the maximum superposition size reaches about $965 \mu\text{m}$ and the initial separation between the wave packets is amplified by a factor of about 1000. Combining the set initial conditions with Eq.(5), (9) and (10), we can obtain a theoretical maximum superposition size of $980 \mu\text{m}$. The disagreement between the analytical and numerical results can be understood by noting that the nanodiamond does not scatter off the magnetic field instantaneously, instead there is a process of deceleration and acceleration. However, since the diamagnetic repulsion is inversely proportional to the third power of the distance (see Eq.(4)), the scattering process mainly takes place very close to the wire. As the scattering process lasts for a very short time, there is not a significant disagreement between the analytical and numerical results.

¹ In reality it is impossible to control the current with a complete precision. As a very good indicator, our current analysis suggests that we will have to limit the current fluctuations, $\delta I/I \lesssim 10^{-9}$, in order to recover the wave packet coherence [28, 53]. However, a detailed analysis will require when we complete the full loop interferometer.

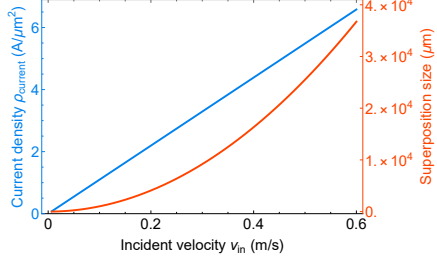


FIG. 2. Superposition size and current density with respect to the incident velocity. The upper blue line shows the current density at different incident velocities when the scattering angle of the nanodiamond is $3\pi/4$. The lower red line shows the superposition size at different incident velocities as the nanodiamond reaches its highest point after being scattered by the magnetic field. Here we have set the impact parameter $b = 0.5 \mu m$.

The closest distance of the wave packet trajectory to the splitting wire is $2.00376 \mu m$, and the closest distance of the wavepacket to the outer reflecting wires (denoted in the plot by left (right) wires, see Fig.1) is $7.67318 \mu m$. If this minimum distance is considered (as an upper limit) to be the maximum radius of the wire, then the current density is $\sim 1 A/\mu m^2$ for the splitting wire, and $\sim 0.2 A/\mu m^2$ for the outer reflecting wires, which is *currently* achievable in a laboratory with carbon nanotubes and graphene [57–59]. The current density through the wire, $\rho_{current}$, the incident velocity of the nanodiamond, v_{in} , and the impact parameter, b , satisfy [54]

$$\rho_{current} = \frac{I}{\pi d^2} = \frac{1}{b} \frac{C v_{in}^2}{\pi (v_{in}^2 + \alpha C^2)}, \quad (12)$$

where $C = I/b$ and d is the closest distance of the wave packet trajectory to the centre of the wire. When the scattering angle is $3\pi/4$, C satisfies Eq.(10) and we have

$$\rho_{current} = \frac{1}{16b\pi} \sqrt{\frac{15}{\alpha}} v_{in}. \quad (13)$$

Note that from Eq.(13) the current density is linear with the incident velocity, as shown in Fig.2. Additionally, the current density is also inversely proportional to the impact parameter b . This means that for a smaller initial separation ($\Delta x_0 = 2b$), we will need a larger current density to achieve the same superposition size.

The relationship between the maximum superposition size and the incident velocity is given by Eq.(9) by taking the scattering angle θ_s to be $3\pi/4$. As can be seen in Fig.2, the superposition size can be increased by an order of magnitude by increasing the incidence velocity with little change in the current density.

Conclusion and discussion: In this paper we have achieved ~ 1000 times increment in the spatial superposition, from $1 \mu m \rightarrow 965 \mu m$ between the

wave packets in 0.034 s by using gravitational acceleration and the repulsive, diamagnetic scattering off the nanodiamond. There are three distinct advantages to this scheme. (1) The first is that the process of enhancing the spatial superposition is *mass independent*. In the ideal situation, when all the known Standard Model interactions are under control along with all the known sources of the decoherence, we can use this mass-independent scheme to increase the spatial superposition between the wave packets $O(10^3) \mu m$, or even higher, provided that we can create an initial spatial superposition, even one as small as $1 \mu m$ or less². This scheme solves some of the outstanding challenges of creating large spatial superposition, either using the wave packet expansions [22, 33, 34, 43–47] or spin-dependent forces [51–53]. In all the previous cases the efficacy is reduced by any increase in the mass. (2) The second advantage is that the whole process takes a very *short time* (around 0.034 s). The shorter time in which one experimental run is performed will reduce the time during which the environment can act to decohere the system. This will also improve the total run-time of the experiment or conversely increase the number of experimental runs performed which is essential for witnessing the entanglement induced by the quantum nature of gravity [24, 25]. (3) The third advantage is that the trajectories of the wave packets can be *recombined* after the separation and the speed of the nanodiamond can be reduced close to zero: *It is a complete “release” and “catch” interferometry scheme*. An advantage of this is that the same high quality nanodiamond, say, with the highest coherence time spin, can be re-used form run to run in this scheme, with mass also remaining same, which could also be relevant for testing the quantum nature of gravity. To get a large enough spatial separation in a short time, it is inevitable that the nanodiamond is accelerated to a relatively large velocity. If this acceleration process utilises spin-dependent forces, then a large magnetic field gradient will be required to achieve this, for example using a magnetic field gradient of $10^4 T/m$ to accelerate the nanodiamond to about 0.1 m/s, see [53]. In this scheme, the separation and closing of the wave packet trajectories can be achieved using a modest current density $O(1) A/\mu m^2$. The ability to restore the spatial superposition to its initial state (even approximately) means that we can use the inverse process of generating the initial spatial separation in the SG apparatus to completely close the trajectories of the wave packets and eventually re-

² Our scheme works even for a smaller initial separation, i.e. for $\Delta x_0 \sim 0.2 \mu m$, a value that could potentially be achieved by a spin dynamical decoupling method for a nanodiamond with a mass of $10^{-17} kg$, see [42]. We can still obtain almost the same maximum superposition size of about $\sim 1000 \mu m$, by a reasonable current density of about $5 A/\mu m^2$.

cover spin coherence [52, 53]. The latter aspects will be discussed separately. In addition to these, there are other issues, such as coherence of the spin in presence of the NV centre [60], or the excitations of the phonons [61]. However, such considerations are left for future study. Since this diamagnetic enhancement does not itself require any spin-based manipulation, there may be simpler candidate for creating (and closing) the initial small spatial splitting which does not

concern itself with the issues of rotation. However it will likely that similar constraints may arise to ensure coherent interference is possible.

Acknowledgements R. Z. is supported by China Scholarship Council (CSC) fellowship. R. J. M. is supported by the Australian Research Council (ARC) under the Centre of Excellence for Quantum Computation and Communication Technology (CE170100012).

[1] F. DYSON, Is a graviton detectable?, *International Journal of Modern Physics A* **28**, 1330041 (2013).

[2] A. Addazi *et al.*, Quantum gravity phenomenology at the dawn of the multi-messenger era—A review, *Prog. Part. Nucl. Phys.* **125**, 103948 (2022), arXiv:2111.05659 [hep-ph].

[3] S. Bose, A. Mazumdar, G. W. Morley, H. Ulbricht, M. Toroš, M. Paternostro, A. A. Geraci, P. F. Barker, M. Kim, and G. Milburn, Spin entanglement witness for quantum gravity, *Physical Review letters* **119**, 240401 (2017).

[4] https://www.youtube.com/watch?v=0Fv-0k13s_k (2016), accessed 1/11/22.

[5] R. J. Marshman, A. Mazumdar, and S. Bose, Locality and entanglement in table-top testing of the quantum nature of linearized gravity, *Physical Review A* **101**, 052110 (2020).

[6] S. Bose, A. Mazumdar, M. Schut, and M. Toroš, Mechanism for the quantum natured gravitons to entangle masses, *Physical Review D* **105**, 106028 (2022).

[7] C. Marletto and V. Vedral, Gravitationally induced entanglement between two massive particles is sufficient evidence of quantum effects in gravity, *Physical Review Letters* **119**, 240402 (2017).

[8] M. Christodoulou and C. Rovelli, On the possibility of laboratory evidence for quantum superposition of geometries, *Physics Letters B* **792**, 64 (2019).

[9] M. Christodoulou, A. Di Biagio, M. Aspelmeyer, Č. Brukner, C. Rovelli, and R. Howl, Locally mediated entanglement through gravity from first principles, arXiv preprint arXiv:2202.03368 (2022).

[10] D. L. Danielson, G. Satishchandran, and R. M. Wald, Gravitationally mediated entanglement: Newtonian field versus gravitons, *Physical Review D* **105**, 086001 (2022).

[11] D. Biswas, S. Bose, A. Mazumdar, and M. Toroš, Gravitational Optomechanics: Photon-Matter Entanglement via Graviton Exchange, (2022), arXiv:2209.09273 [gr-qc].

[12] D. Carney, Newton, entanglement, and the graviton, *Phys. Rev. D* **105**, 024029 (2022), arXiv:2108.06320 [quant-ph].

[13] T. W. van de Kamp, R. J. Marshman, S. Bose, and A. Mazumdar, Quantum Gravity Witness via Entanglement of Masses: Casimir Screening, *Phys. Rev. A* **102**, 062807 (2020), arXiv:2006.06931 [quant-ph].

[14] M. Toroš, T. W. Van De Kamp, R. J. Marshman, M. S. Kim, A. Mazumdar, and S. Bose, Relative acceleration noise mitigation for nanocrystal matter-wave interferometry: Applications to entangling masses via quantum gravity, *Phys. Rev. Res.* **3**, 023178 (2021), arXiv:2007.15029 [gr-qc].

[15] R. Penrose, On gravity's role in quantum state reduction, *General relativity and gravitation* **28**, 581 (1996).

[16] L. Diósi, Continuous Quantum Measurement and Ito Formalism, *Phys. Lett. A* **129**, 419 (1988), arXiv:1812.11591 [quant-ph].

[17] P. Pearle, Combining stochastic dynamical state-vector reduction with spontaneous localization, *Physical Review A* **39**, 2277 (1989).

[18] A. Bassi, K. Lochan, S. Satin, T. P. Singh, and H. Ulbricht, Models of wave-function collapse, underlying theories, and experimental tests, *Reviews of Modern Physics* **85**, 471 (2013).

[19] S. Nimmrichter and K. Hornberger, Macroscopicity of mechanical quantum superposition states, *Physical Review Letters* **110**, 160403 (2013).

[20] S. Bose, A. Mazumdar, M. Schut, and M. Toroš, Entanglement Witness for the Weak Equivalence Principle, (2022), arXiv:2203.11628 [gr-qc].

[21] O. Romero-Isart, Quantum superposition of massive objects and collapse models, *Phys. Rev. A* **84**, 052121 (2011).

[22] O. Romero-Isart, A. C. Pflanzer, F. Blaser, R. Kaltenbaek, N. Kiesel, M. Aspelmeyer, and J. I. Cirac, Large quantum superpositions and interference of massive nanometer-sized objects, *Physical Review Letters* **107**, 020405 (2011).

[23] O. Romero-Isart, M. L. Juan, R. Quidant, and J. I. Cirac, Toward quantum superposition of living organisms, *New Journal of Physics* **12**, 033015 (2010).

[24] J. Tilly, R. J. Marshman, A. Mazumdar, and S. Bose, Qudits for witnessing quantum-gravity-induced entanglement of masses under decoherence, *Phys. Rev. A* **104**, 052416 (2021), arXiv:2101.08086 [quant-ph].

[25] M. Schut, J. Tilly, R. J. Marshman, S. Bose, and A. Mazumdar, Improving resilience of quantum-gravity-induced entanglement of masses to decoherence using three superpositions, *Phys. Rev. A* **105**, 032411 (2022), arXiv:2110.14695 [quant-ph].

[26] S. Rijavec, M. Carlesso, A. Bassi, V. Vedral, and C. Marletto, Decoherence effects in non-classicality tests of gravity, *New J. Phys.* **23**, 043040 (2021), arXiv:2012.06230 [quant-ph].

[27] D. Carney, P. C. E. Stamp, and J. M. Taylor, Tabletop experiments for quantum gravity: a user's manual, *Classical and Quantum Gravity* **36**, 034001 (2019).

[28] R. J. Marshman, A. Mazumdar, G. W. Morley, P. F. Barker, S. Hoekstra, and S. Bose, Mesoscopic Interference for Metric and Curvature (MIMAC) & Gravitational Wave Detection, *New J. Phys.* **22**, 083012 (2020), arXiv:1807.10830 [gr-qc].

[29] P. F. Barker, S. Bose, R. J. Marshman, and A. Mazumdar, Entanglement based tomography to probe new macroscopic forces, *Phys. Rev. D* **106**, L041901 (2022), arXiv:2203.00038 [hep-ph].

[30] J. M. McGuirk, G. T. Foster, J. B. Fixler, M. J. Snadden, and M. A. Kasevich, Sensitive absolute-gravity gradiometry using atom interferometry, *Physical Review A* **65**, 033608 (2002).

[31] S. Dimopoulos, P. W. Graham, J. M. Hogan, and M. A. Kasevich, General relativistic effects in atom interferometry, *Physical Review D* **78**, 042003 (2008).

[32] P. Asenbaum, C. Overstreet, T. Kovachy, D. D. Brown, J. M. Hogan, and M. A. Kasevich, Phase shift in an atom interferometer due to spacetime curvature across its wave function, *Physical Review Letters* **118**, 183602 (2017).

[33] M. Arndt, O. Nairz, J. Vos-Andreae, C. Keller, G. van der Zouw, and A. Zeilinger, Wave-particle duality of C_{60} molecules, *Nature* **401**, 680 (1999).

[34] S. Gerlich, S. Eibenberger, M. Tomandl, S. Nimmrichter, K. Hornberger, P. J. Fagan, J. Tüxen, M. Mayor, and M. Arndt, Quantum interference of large organic molecules, *Nature communications* **2**, 1 (2011).

[35] S. Bose, K. Jacobs, and P. L. Knight, A Scheme to probe the decoherence of a macroscopic object, *Phys. Rev. A* **59**, 3204 (1999), arXiv:quant-ph/9712017.

[36] P. Sekatski, M. Aspelmeyer, and N. Sangouard, Macroscopic optomechanics from displaced single-photon entanglement, *Physical Review Letters* **112**, 080502 (2014).

[37] J. M. Hogan, D. Johnson, and M. A. Kasevich, Light-pulse atom interferometry, arXiv preprint arXiv:0806.3261 (2008).

[38] C. Wan, M. Scala, G. Morley, A. A. Rahman, H. Ulbricht, J. Bateman, P. Barker, S. Bose, and M. Kim, Free nano-object ramsey interferometry for large quantum superpositions, *Physical Review Letters* **117**, 143003 (2016).

[39] M. Scala, M. S. Kim, G. W. Morley, P. F. Barker, and S. Bose, Matter-wave interferometry of a levitated thermal nano-oscillator induced and probed by a spin, *Physical Review Letters* **111**, 180403 (2013).

[40] Z.-q. Yin, T. Li, X. Zhang, and L. Duan, Large quantum superpositions of a levitated nanodiamond through spin-optomechanical coupling, *Physical Review A* **88**, 033614 (2013).

[41] J. Clarke and M. R. Vanner, Growing macroscopic superposition states via cavity quantum optomechanics, *Quantum Science and Technology* **4**, 014003 (2019).

[42] B. D. Wood, S. Bose, and G. W. Morley, Spin dynamical decoupling for generating macroscopic superpositions of a free-falling nanodiamond, *Physical Review A* **105**, 012824.

[43] R. Kaltenbaek, M. Aspelmeyer, P. F. Barker, A. Bassi, J. Bateman, K. Bongs, S. Bose, C. Braxmaier, C. Brukner, B. Christophe, et al., Macroscopic quantum resonators (maqro): 2015 update, *EPJ Quantum Technology* **3**, 5 (2016).

[44] H. Pino, J. Prat-Camps, K. Sinha, B. P. Venkatesh, and O. Romero-Isart, On-chip quantum interference of a superconducting microsphere, *Quantum Science and Technology* **3**, 025001 (2018).

[45] O. Romero-Isart, Coherent inflation for large quantum superpositions of levitated microspheres, *New Journal of Physics* **19**, 123029 (2017).

[46] R. Kaltenbaek, G. Hechenblaikner, N. Kiesel, O. Romero-Isart, K. C. Schwab, U. Johann, and M. Aspelmeyer, Macroscopic quantum resonators (maqro), *Experimental Astronomy* **34**, 123 (2012).

[47] M. Arndt and K. Hornberger, Testing the limits of quantum mechanical superpositions, *Nature Physics* **10**, 271 (2014).

[48] S. Machluf, Y. Japha, and R. Folman, Coherent stern-gerlach momentum splitting on an atom chip, *Nature Communications* **4**, 2424 (2013).

[49] O. Amit, Y. Margalit, O. Dobkowski, Z. Zhou, Y. Japha, M. Zimmermann, M. A. Efremov, F. A. Narducci, E. M. Rasel, W. P. Schleich, and R. Folman, T^3 stern-gerlach matter-wave interferometer, *Physical Review Letters* **123**, 083601 (2019).

[50] Y. Margalit, Z. Zhou, O. Dobkowski, Y. Japha, D. Rohrlich, S. Moukouri, and R. Folman, Realization of a complete stern-gerlach interferometer, arXiv preprint arXiv:1801.02708 (2018).

[51] Y. Margalit, O. Dobkowski, Z. Zhou, O. Amit, Y. Japha, S. Moukouri, D. Rohrlich, A. Mazumdar, S. Bose, C. Henkel, and R. Folman, Realization of a complete stern-gerlach interferometer: Toward a test of quantum gravity, *Science Advances* **7**, 10.1126/sci-adv.2879 (2021).

[52] R. J. Marshman, A. Mazumdar, R. Folman, and S. Bose, Constructing nano-object quantum superpositions with a Stern-Gerlach interferometer, *Phys. Rev. Res.* **4**, 023087 (2022), arXiv:2105.01094 [quant-ph].

[53] R. Zhou, R. J. Marshman, S. Bose, and A. Mazumdar, Catapulting towards massive and large spatial quantum superposition, (2022), arXiv:2206.04088 [quant-ph].

[54] R. Zhou, R. J. Marshman, S. Bose, and A. Mazumdar, Mass Independent Scheme for Large Spatial Quantum Superpositions, (2022), arXiv:2210.05689 [quant-ph].

[55] F. Shi, X. Kong, P. Wang, F. Kong, N. Zhao, R.-B. Liu, and J. Du, Sensing and atomic-scale structure analysis of single nuclear-spin clusters in diamond, *Nature Physics* **10**, 21 (2014).

[56] E. V. Levine, M. J. Turner, P. Kehayias, C. A. Hart, N. Langellier, R. Trubko, D. R. Glenn, R. R. Fu, and R. L. Walsworth, Principles and techniques of the quantum diamond microscope, *Nanophotonics* **8**, 1945 (2019).

[57] Z. Yao, C. L. Kane, and C. Dekker, High-field electrical transport in single-wall carbon nanotubes, *Physical Review Letters* **84**, 2941 (2000).

[58] B. Q. Wei, R. Vajtai, and P. M. Ajayan, Reliability and current carrying capacity of carbon nanotubes, *Applied Physics Letters* **79**, 1172 (2001).

[59] R. Murali, Y. Yang, K. Brenner, T. Beck, and J. D. Meindl, Breakdown current density of graphene nanoribbons, *Applied Physics Letters* **94**, 243114

(2009).

[60] Y. Japha and R. Folman, Role of rotations in stern-gerlach interferometry with massive objects 10.48550/arxiv.2202.10535 (2022).

[61] C. Henkel and R. Folman, Internal decoherence in nano-object interferometry due to phonons, AVS Quantum Sci. **4**, 025602 (2022), arXiv:2112.01263 [quant-ph].